

# Isothermal crystallization behaviors and kinetics of nucleated polylactide/poly(butylene adipate-co-terephthalate) blend films with talc

## Influence of compatibilizer contents

Worasak Phetwarotai<sup>1,2</sup> · Duangdao Aht-Ong<sup>1,2</sup>

Received: 16 March 2016 / Accepted: 24 June 2016 / Published online: 6 July 2016  
© Akadémiai Kiadó, Budapest, Hungary 2016

**Abstract** Polylactide (PLA) and its blend films with and without a compatibilizer in the presence of poly(butylene adipate-co-terephthalate) (PBAT) and talc were prepared through a twin-screw extruder. The effects of PBAT, talc, and various contents of compatibilizer on thermal and morphological properties as well as crystallization of these blends were investigated. PBAT and talc were used as a flexible polymer and a nucleating agent at 10 mass% and 1 phr, respectively, whereas methylenediphenyl diisocyanate was used as a compatibilizer at different amounts (1–7 mass% based on PBAT contents). Isothermal crystallization behaviors and kinetics of neat and nucleated PLA blends were evaluated by differential scanning calorimeter and polarized optical microscope. The Avrami and Arrhenius equations were used to investigate the crystallization kinetics. The results revealed that the presence of PBAT and talc in the films led to an increment of crystallization rate of PLA via a synergistic effect under isothermal crystallization conditions. However, the crystallization rate significantly decreased with increasing the crystallization temperature ( $T_c$ ). These results were in agreement with crystallization kinetic and morphological studies, suggesting that the crystallization behaviors, kinetics, and mechanisms of PLA were affected by these factors.

**Keywords** Biodegradable polymers · Polylactide · Isothermal crystallization · Kinetic · Compatibilizer · Film

## Introduction

Poly(lactide) or poly(lactic acid), a linear aliphatic polyester, is well known in the name of PLA. Generally, it is synthesized through ring-opening polymerization of lactides or direct condensation processes of lactic acid monomers which are derived from the fermentation of sugar feed stocks [1, 2]. In the present, PLA is one of the most popular biodegradable polymers due to several excellent reasons; high mechanical strength, renewable product, biocompatibility, fully biodegradation within a few weeks, transparency, gas permeability, and easy processability [3–5]. According to these advantages, PLA which can be potentially applied in many fields such as tissue engineering, drug delivery system, automobile, food container, and film packaging becomes a promising and outstanding bio-based material for replacing petroleum-based plastics, e.g., polyolefins (PE and PP), polystyrene (PS), and poly(ethylene terephthalate) (PET) as well [6–8].

Unfortunately, the shortcomings of PLA which overshadows its remarkable properties and limits its application range are low crystallinity, slow crystallization rate, and brittleness [9, 10]. To overcome these drawbacks, many researches have been studied about PLA blending with a nucleating agent and a flexible polymer for improving the crystallization behavior and toughness of PLA. Many attempts have revealed that the nucleating agents such as modified montmorillonite (MMT), clay, and talc as well as the flexible polymer such as poly( $\epsilon$ -caprolactone) (PCL) and poly(butylene adipate-co-terephthalate) (PBAT) have been well-worked with PLA [4, 5, 11, 12]. One of the most

✉ Duangdao Aht-Ong  
duangdao.a@chula.ac.th

<sup>1</sup> Department of Materials Science, Faculty of Science, Chulalongkorn University, Bangkok 10330, Thailand

<sup>2</sup> Center of Excellence on Petrochemical and Materials Technology, Chulalongkorn University, Bangkok 10330, Thailand

widely studied and effective nucleating agents and flexible polymers for PLA modification are talc and PBAT, respectively, which have been used to enhance the crystallization rate, nucleation density, impact strength, and flexibility of the blends [5, 11]. However, incompatibility of PLA and PBAT phases leads to poor mechanical properties especially low elongation at break of the PLA/PBAT blends.

In order to enhance an interfacial adhesion between two phases of PLA and PBAT, a compatibilizer which could react with both functional groups of matrix and filler should be added into the blend system at appropriate content. For example, several efficient compatibilizers such as dioctyl maleate (DOM) [13], maleic anhydride (MA) [14, 15], PLA-graft-maleic anhydride (PLA-g-MA) [16, 17], and methylenediphenyl diisocyanate (MDI) [18–20] have been studied and used to compatibilize with the PLA blends. Methylenediphenyl diisocyanate (MDI) is one of the most powerful compatibilizers that can strongly improve the interfacial strength of PLA and its blends [20]. In cases of the crystallization behavior and kinetic studies, the influences of many additives such as nucleating agent, plasticizer, and filler on PLA have been widely investigated either alone or in combination with each other. For example, Li and Huneault [21] have investigated the effects of nucleating agent and plasticizer on the PLA crystallization. Talc, sodium stearate, and calcium lactate were used as potential nucleating agents, while acetyl triethyl citrate (ATC) and poly(ethylene glycol) (PEG) were acted as plasticizers. Crystallization kinetics of PLA have been studied in both isothermal and non-isothermal conditions. The results indicated that the crystallinity of PLA was significantly improved at high cooling rate when the nucleating agent and plasticizer were used [21]. Recently, Lee and Jeong have studied the crystallization behaviors of PLA nanocomposites reinforced with polyhedral oligomeric silsesquioxane-modified MMT (POSS–MMT). The influence of POSS–MMT as a nucleating agent was emphasized. They reported that

the crystallization rate of PLA/POSS–MMT nanocomposites was highly enhanced by the presence of POSS–MMT nanoparticles dispersed thoroughly in PLA matrix [22].

Surprisingly, to our knowledge, not many researches have been reported on the influences of a compatibilizer on the isothermal crystallization behaviors and kinetics of PLA and its blends, particularly with the presence of nucleating agent. As a result, the objectives of this work were focused on the effects of PBAT, talc, and various contents of MDI on the thermal and morphological properties including isothermal crystallization behaviors and kinetics of neat and nucleated PLA blend films. In this research, PBAT, talc, and MDI were used as a flexible polymer, a nucleating agent, and a compatibilizer for PLA blend films, respectively.

## Experimental

### Materials

The commercial PLA resin (PLA 4042D) purchased from NatureWork LLC (Cargill-Dow, Minneapolis, MN) was used as a polymer matrix. PLA pellets were transparent with a density of  $1.24 \text{ g cm}^{-3}$  reported by the manufacturer. Glass transition temperature ( $T_g$ ) and melting temperature ( $T_m$ ) characterized by differential scanning calorimeter (DSC) analysis were about 60 and 153 °C, respectively. Weight average molecular weight and polydispersity (PDI) of PLA determined by gel permeation chromatography (GPC) in tetrahydrofuran (THF) were 130 kDa and 1.46, respectively. PBAT (Ecoflex F BX7011) with a density of  $1.26 \text{ g cm}^{-3}$  was purchased from BASF Corporation (Ludwigshafen, Germany). The  $T_g$  and  $T_m$  of PBAT characterized by DSC were about –30 and 110 °C, while its weight average molecular weight and PDI values were 170 kDa and 1.32 (GPC analysis in THF), respectively. Talc with a volume mean diameter of 19.03  $\mu\text{m}$  analyzed by mastersizer was supplied from Siam

**Table 1** Formulations of neat PLA and nucleated PLA/PBAT blend films with talc and MDI

Sample ID	Compositions			
	PLA/mass%	PBAT/mass%	Talc/phr	MDI/mass% based on PBAT content
PLA	100	–	–	–
PLA_PB 90_10	90	10	–	–
PLA_PB_Ta 90_10_1	90	10	1	–
PLA_PB_Ta_MD 90_10_1_1	90	10	1	1
PLA_PB_Ta_MD 90_10_1_3	90	10	1	3
PLA_PB_Ta_MD 90_10_1_5	90	10	1	5
PLA_PB_Ta_MD 90_10_1_7	90	10	1	7

Cement Group (SCG Chemicals) Co., Ltd., Rayong, Thailand. MDI was obtained from Siam Chemical Industry Co., Ltd., Bangkok, Thailand.

### Blend preparation

The PLA, PBAT, and talc were dried in vented oven at 60 °C overnight before usage and stored in a desiccator. Talc and MDI acted as a nucleating agent for accelerating crystallization rate and a compatibilizer for improving interfacial adhesion of the PLA/PBAT blend films, respectively. The PLA was blended with PBAT at the mass ratio of 90–10 for all experiments. The amount of talc was fixed at 1 phr, whereas MDI contents were varied from 0 to 7 mass% based on PBAT content. The mixtures of PLA, PBAT, talc, and MDI were premixed in zip-lock plastic bag before extrusion process. The nucleated PLA blends were prepared directly in a corotating twin-screw extruder (PRISM TSE 16TC, Thermo Electron, Staffordshire, UK) on five zones along the extrusion barrel and a strand die (screw diameter = 15.6 mm,  $L/D$  ratio = 40, temperature profile = 120–190 °C, and screw speed = 60 rpm). The extruded materials were then cooled in water and pelletized into the blend pellets. The pellets were dried in vented oven overnight and then compression-molded using a hydraulic press (Scientific, Labtech Engineering, Samutprakarn, Thailand) under optimum conditions; temperature, holding pressure, and time of 180 °C, 1500 psi, and 15 min, respectively. The neat PLA was also taken in the same way in order to be used as a reference material. The sample formulations were listed in Table 1.

### Gel permeation chromatography (GPC)

The gel permeation chromatography systems (GPC; 10A series, Shimadzu, Japan) were composed of the following units: LC-10ATVP Shimadzu solvent delivery system, a SIL-10ADVP Shimadzu auto-injector, a column set which consisted of a PL 5.0- $\mu\text{m}$  bead size guard column and a set of 5.0- $\mu\text{m}$  PL linear columns (103, 104, 105 Å) kept at a constant temperature of 40 °C inside a CTO-10AC VP Shimadzu Column Oven, and a RID-10A Shimadzu refractive index detector. The GPC was used to determine molecular weight and polydispersity index (PDI) of neat PLA and PBAT. This process was done by first analyzing a series of standards of known molecular weight. The retention time for these standards was then used to create a calibration curve. Polystyrene (PS) was used for calibration, whereas tetrahydrofuran (THF) was utilized as the continuous phase. Test specimen was prepared by dissolving 50 mg of sample powder in THF. The temperature and flow rate were used as 25 °C and 1 mL  $\text{min}^{-1}$ , respectively.

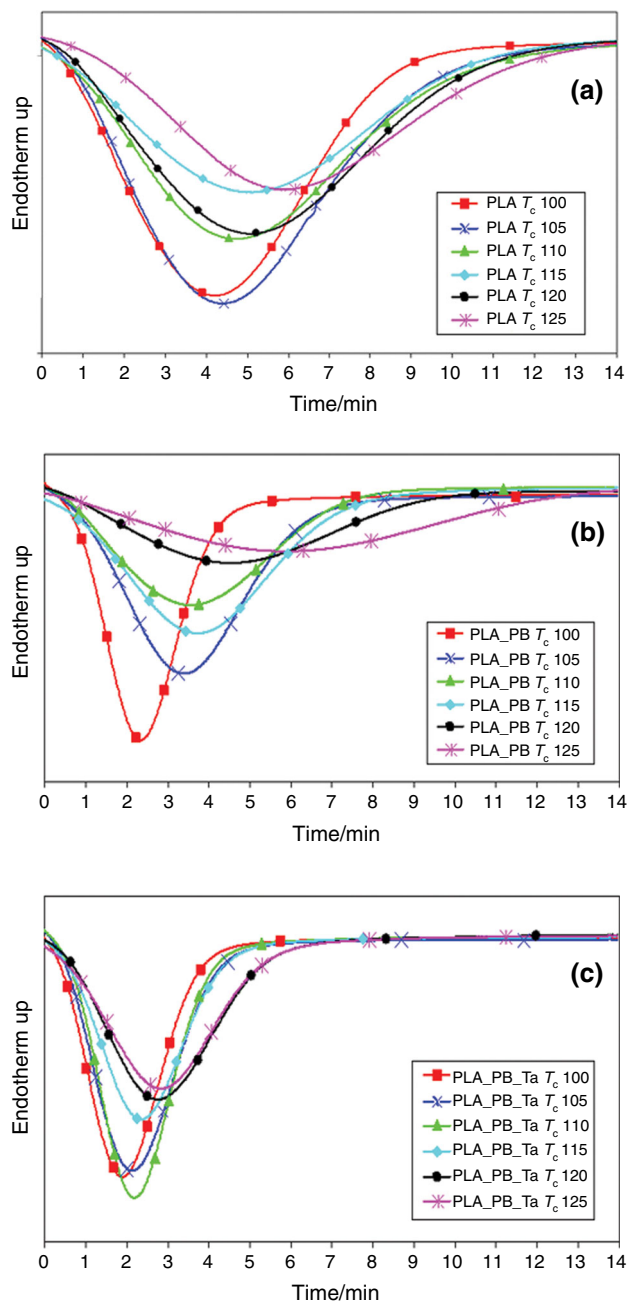


**Fig. 1** DSC curves of isothermal crystallization exotherm of a neat PLA, b PLA/PBAT (90/10), and c PLA/PBAT/talc (90/10/1) blend films at different crystallization temperatures (100–125 °C)

### Particle size distribution

Particle size distribution of talc was investigated by Mastersizer (S long bed Ver. 2.19, Malvern Instruments Ltd., Worcestershire, UK). The relative volume distribution of both wet and dry samples can be detected, based on a diffraction of a laser beam under a particle size ranging from 0.01 to 3500  $\mu\text{m}$ . Sample solution which was prepared by dissolving 1 mg of sample in ethanol (100 mL)

was homogenized and deagglomerated in ultrasonic technique for 10 min before measuring the particle size distribution.

### Thermal analysis

The thermal behaviors of neat PLA and its blends were evaluated using a differential scanning calorimeter (Pyris Diamond DSC, PerkinElmer, Waltham, MA). Approximately 6–8 mg of samples was encapsulated in a hermetically sealed aluminum pan (30  $\mu\text{L}$ ) for each experiment. The first heating scan was operated from room temperature to 200  $^{\circ}\text{C}$  at a heating rate of 10  $^{\circ}\text{C min}^{-1}$  and held at 200  $^{\circ}\text{C}$  for 3 min to get rid of any thermal history of all samples. Then, the sample was rapidly cooled by using liquid nitrogen to  $-50^{\circ}\text{C}$ . Finally, the second heating scan was heated to 200  $^{\circ}\text{C}$  at a heating rate of 10  $^{\circ}\text{C min}^{-1}$  to determine the actual thermal characteristics of the films. All experiments were operated under nitrogen atmosphere.

### Isothermal crystallization experiment

The DSC technique was also used to study the effect of PBAT, talc, and various contents of MDI on the isothermal crystallization behaviors and kinetics of the neat and nucleated PLA blend films. The sample of about 6–8 mg

was cut from the blend films and sealed in a hermetically sealed aluminum pan (30  $\mu\text{L}$ ) for each experiment. Then, it was melted at 200  $^{\circ}\text{C}$  and remained at that temperature for 3 min to erase the thermal history of all samples. To determine isothermal crystallization behaviors and kinetics of the films, the melted sample was rapidly cooled from 200  $^{\circ}\text{C}$  to an indicated isothermal crystallization temperature ( $T_c$ ) and held at that temperature until crystallization completed. The indicated  $T_c$ s were 100, 105, 110, 115, 120, and 125  $^{\circ}\text{C}$ . The range of indicated  $T_c$  for isothermal crystallization was selected from our previous work which was carried out under non-isothermal crystallization behaviors of neat and nucleated PLA blend films [23]. Relative crystallization ( $X_t$ ), crystallization time ( $t$ ), crystallization half-time ( $t_{1/2}$ ), crystallization rate constant ( $K$ ), Avrami exponent ( $n$ ), and activation energy ( $\Delta E_a$ ) were used to evaluate the isothermal crystallization behaviors and kinetics of neat and nucleated PLA blend films with the presence of PBAT, talc, and different amounts of MDI.

### Polarized optical microscope (POM)

A polarized optical microscope (POM; DFC295, Leica Microsystems Ltd., Wetzlar, Germany) equipped with a hot stage (FP82HT, Mettler-Toledo, Greifensee, Switzerland) was used to observe and determine the nucleation and

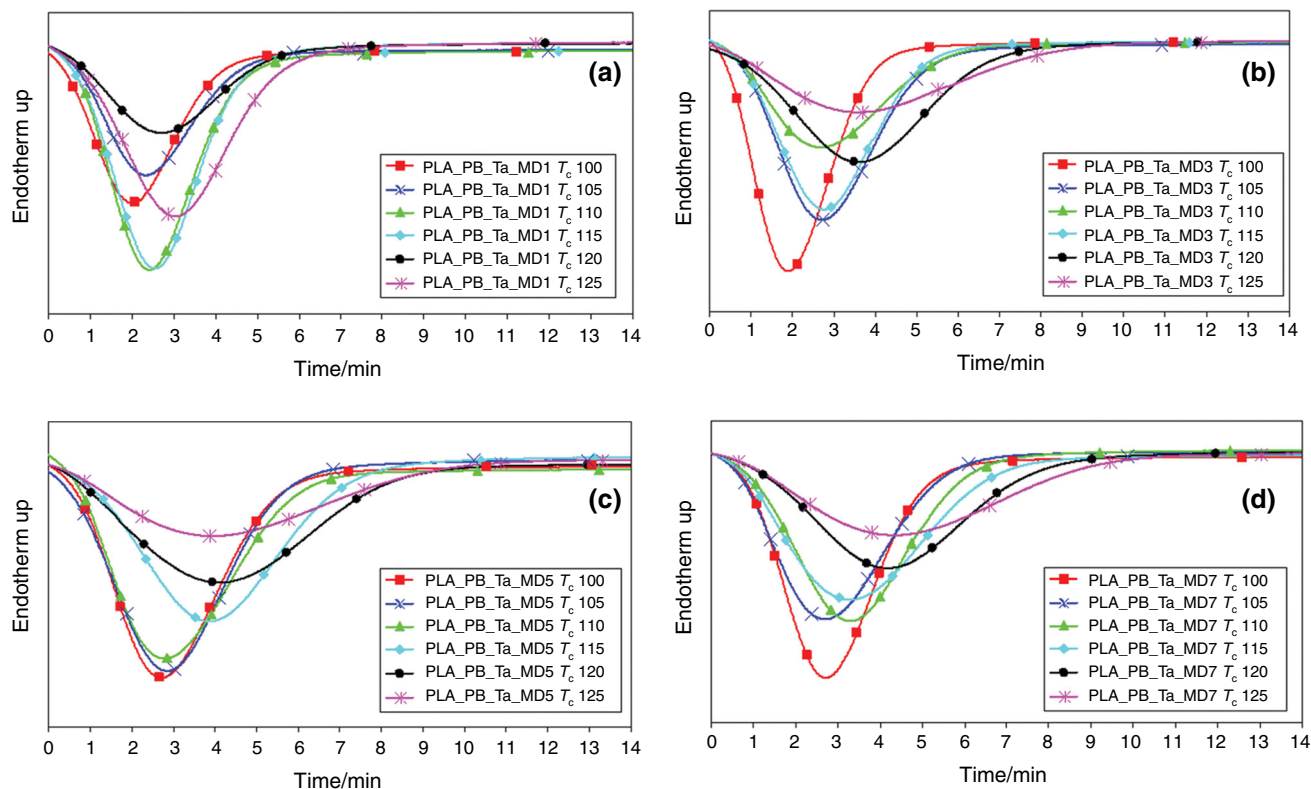


**Fig. 2** DSC curves of isothermal crystallization exotherm of PLA/PBAT/Talc (90/10/1) blend films with **a** 1 %, **b** 3 %, **c** 5 %, and **d** 7 % MDI based on PBAT contents

isothermal crystallization behaviors of neat and nucleated PLA blend films. The obtained POM micrographs revealed the changes of crystal size, spherulitic morphology, nucleation density, and crystallization rate of the blend films under the influences of PBAT, talc, and various levels of MDI. The test specimen was firstly placed between cover and glass slides. After that, the sample was moved to the hot stage where the temperature was set at 200 °C for melting the films and kept at this temperature for 3 min. It was finally quenched to an indicated  $T_c$  (100–125 °C) and maintained at that indicated  $T_c$  for evaluating the crystallization behaviors of the films as a function of crystallization time. The POM methods were carried out as similar circumstance as the isothermal crystallization evaluation in DSC technique.

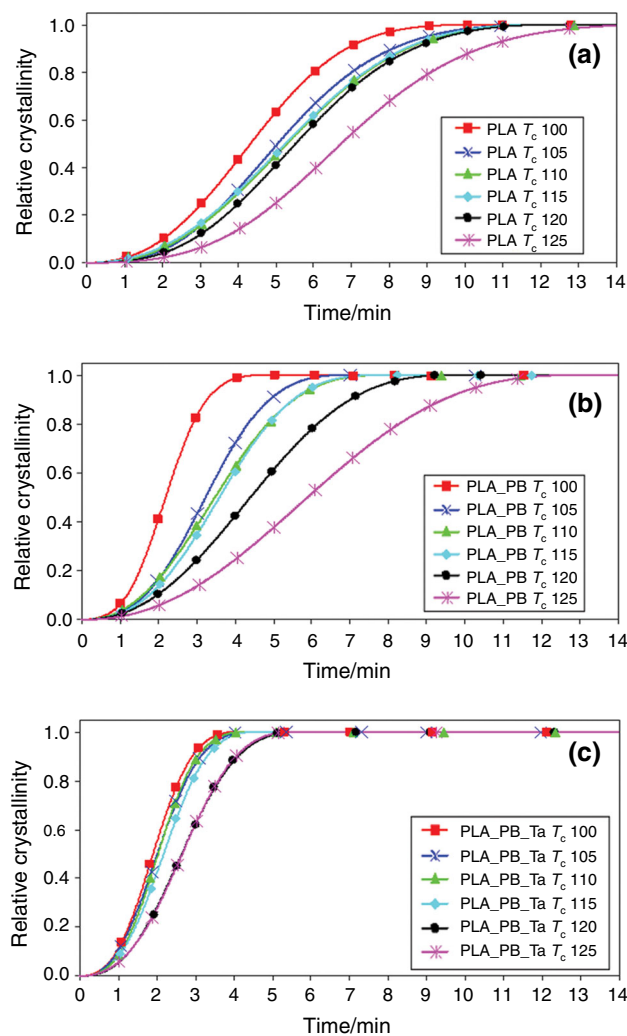
## Results and discussion

### Isothermal crystallization behaviors and kinetics

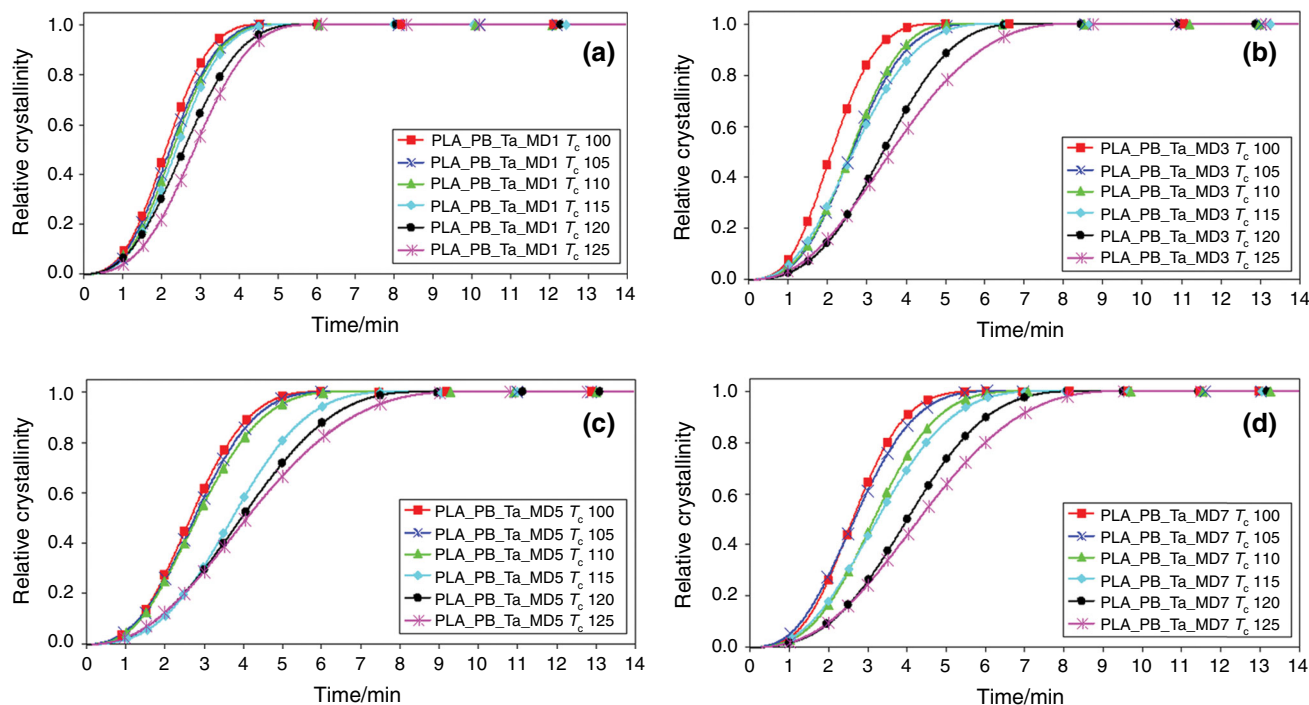
The DSC technique was utilized to evaluate isothermal crystallization behaviors and kinetics of PLA and its blend films at different crystallization temperatures ( $T_c$ ) which were in the range of 100–125 °C. The data from DSC curves can be used to calculate and determine the relative crystallization ( $X_t$ ), crystallization time ( $t$ ), crystallization half-time ( $t_{1/2}$ ), crystallization rate constant ( $K$ ), Avrami exponent ( $n$ ), and activation energy ( $\Delta E_a$ ) based on Avrami and Arrhenius models in order to understand the isothermal crystallization behaviors and kinetics of neat PLA and its blends in the presence of PBAT, talc, and different amounts of MDI.

Figure 1 represents the DSC curves of isothermal crystallization exotherm of neat PLA and PLA/PBAT (90/10 w/w) blend films with and without talc at the indicated  $T_c$  ranging from 100 to 125 °C. In Fig. 1a, the isothermal crystallization exotherms of neat PLA indicated that the exothermic peaks were broader when they were isothermally crystallized at higher  $T_c$ . In contrast, those were narrowed at lower  $T_c$ . These results exhibited that the isothermal crystallization rate of neat PLA was slower with the increasing of  $T_c$ . Similar behaviors were demonstrated in both PLA/PBAT (90/10 w/w) blend films with and without talc (Fig. 1b, c). However, the exothermic peaks of PLA blend films were apparently narrowed with the addition of PBAT and talc at all conditions. These results indicated that crystallization time of PLA became faster with the presence of 10 mass% PBAT in the blend films. Furthermore, Fig. 1c shows an interestingly synergistic effect of PBAT and talc leading to a significant reduction of crystallization time for isothermal crystallization of PLA at various  $T_c$ s.

Figure 2 indicates the influences of various MDI contents on the isothermal crystallization exotherms of PLA/PBAT/talc (90/10/1) blend films. These results showed that the exothermic peaks of the blend films depended on the different  $T_c$ s and MDI contents. When the  $T_c$  increased, the crystallization time of nucleated PLA blend films with MDI evidently prolonged especially at indicated  $T_c$  of 125 °C. As shown in Fig. 2c and 2d, the negative effect on the isothermal crystallization rate of nucleated PLA blend films with higher amount of MDI (5 and 7 mass%) was clearly observed. It means that a higher amount of MDI led to longer crystallization time of the PLA blend films compared to the lower ones (1 and 3 mass%). The isothermal crystallization rate of neat and nucleated PLA blend films at each  $T_c$  can be obviously evaluated by value of crystallization half-time



**Fig. 3** Relative crystallization ( $X_t$ ) as a function of crystallization time at various crystallization temperatures (100–125 °C) for isothermal crystallization of **a** neat PLA, **b** PLA/PBAT (90/10), and **c** PLA/PBAT/talc (90/10/1) blend films



**Fig. 4** Relative crystallization ( $X_t$ ) as a function of crystallization time at various crystallization temperatures (100–125 °C) for isothermal crystallization of PLA/PBAT/talc (90/10/1) blend films with **a** 1 %, **b** 3 %, **c** 5 %, and **d** 7 % MDI based on PBAT contents

( $t_{1/2}$ ). The details of this parameter will be explained in the next section. Despite the addition of MDI, the isothermal crystallization rate of nucleated PLA blend films was still faster than that of neat PLA (Fig. 1a). It might be implied that the influences of PBAT and talc on the isothermal crystallization behaviors of PLA were more significant than those of MDI. For easy understanding about the relationship between relative crystallinity ( $X_t$ ) and crystallization time, raw data from Figs. 1 and 2 were used to analyze and create the plots of  $X_t$  as a function of crystallization time at various  $T_c$ s as shown in Figs. 3 and 4, respectively. The  $X_t$  was calculated by Eq. (1) [22].

$$X_t = \frac{\int_{t_0}^t (dH_c/dT)dT}{\int_{t_0}^{t_\infty} (dH_c/dT)dT} \quad (1)$$

where  $t_0$  and  $t_\infty$  are beginning and end times of crystallization, respectively. The slope of graphs shown in Figs. 3 and 4 is appeared as S-like shape. These results can be used to evaluate the crystallization rate of the neat and nucleated PLA blends. The S-like shape in graphs with higher slope revealed higher rate changes of relative crystallization versus time, indicating a faster rate of crystallization. It can be seen that the slope of S-like-shaped graphs depended evidently on the increasing of  $T_c$  and the presence of PBAT, talc, as well as MDI. For example, from Fig. 3 at  $X_t$  value of 0.3 and  $T_c$  of 100 °C, the crystallization time of neat PLA, PLA/PBAT (90/10 w/w) with and without talc

was 3.3, 1.8, and 1.5 min, respectively. These experimental values showed that the faster crystallization of PLA was associated with the addition of PBAT and talc. These behaviors could be explained in the same way Figs. 1 and 2. It can be summarized that (1) the crystallization rate of neat PLA and its blends was prolonged with the increasing  $T_c$ , (2) the presence of PBAT and talc showed a synergistic effect on the accelerating isothermal crystallization of PLA, and (3) the different levels of MDI on the blend films led to retardation on the crystallization rate of PLA.

As mentioned above, to compare the effects of PBAT, talc, and various MDI contents on the crystallization rate for each sample, the plots of  $t_{1/2}$  derived from the plots between  $X_t$  and time (Figs. 3, 4) as a function of  $T_c$  are evaluated as shown in Fig. 5. The  $t_{1/2}$  which is defined as the time at which the degree of crystallization is 50 % can be inversely used to determine the rate of crystallization [24]. The  $t_{1/2}$  data of neat PLA and its blends are listed in Table 2. The results showed that  $t_{1/2}$  of neat PLA raised significantly with the increasing of  $T_c$  especially at  $T_c$  of 125 °C, while the addition of PBAT, talc, and MDI in the blend films led to the depression of  $t_{1/2}$  values. For example, the  $t_{1/2}$  values of neat PLA and PLA/PBAT/talc (90/10/1) blend films were 4.3 and 1.9 min at  $T_c$  of 100 °C, whereas those values were found to be 6.7 and 2.7 min at  $T_c$  of 125 °C, respectively. These results indicated that crystallization rate of PLA/PBAT (90/10 w/w) blend films with talc was almost 2.5-fold faster than that of neat PLA at

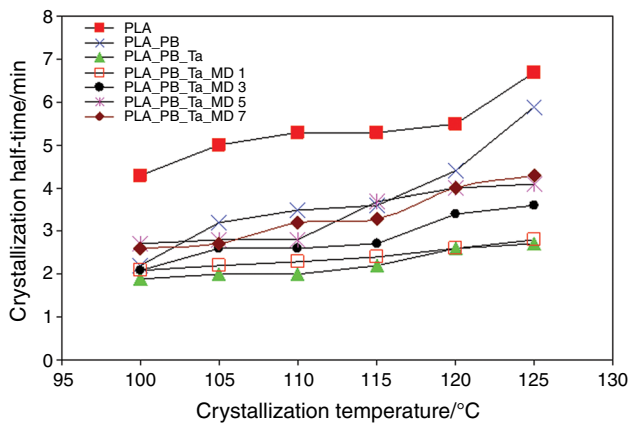


**Fig. 5** Plots of crystallization half-time ( $t_{1/2}$ ) as a function of crystallization temperature ( $T_c$ ) for isothermal crystallization of neat PLA and nucleated PLA blend films with and without MDI content

$T_c$  of 125 °C. Nevertheless, the different values of  $t_{1/2}$  for neat PLA and nucleated PLA/PBAT blend films were decreased with the increment of MDI amounts as evidently observed by POM morphological results. From the experimental data, the addition of PBAT and talc could accelerate the crystallization rate of PLA (i.e.,  $t_{1/2}$  decreased) in contrast to the presence of MDI. These behaviors might be explained by three possible reasons. First, the presence of

flexible polymer like a PBAT contributed to an increment of chain mobility of PLA matrix [25]. Hence, the rigidity and  $T_g$  of PLA chains were reduced, leading to crystallinity enhancement. Secondly, talc which acted as a nucleating agent driven a great number of nuclei and spherulitic sites into melted PLA and then attributed to higher nucleation density and crystal formation. Finally, MDI might be a chain extender between PLA and PBAT resulting in longer polymer chains and higher chain rigidity. As a result, the crystallization rate of PLA was prolonged (i.e.,  $t_{1/2}$  increased) with the addition of MDI.

Generally, the Avrami equation which explains the time evolution of overall crystallinity can be applied to any types of crystallization and is not restricted only to polymers [26]. As a result, in this research, the isothermal crystallization kinetics of neat and nucleated PLA blend films were evaluated by using Avrami model according to the following Eq. (2):

$$1 - X_t = \exp(-Kt^n) \tag{2}$$

where  $X_t$  is the relative crystallinity depended on time,  $t$  is crystallization time,  $K$  is crystallization rate constant, and  $n$  is Avrami exponent which related to nucleation and crystal growth geometry [22]. The Avrami Eq. (2) can be rearranged into the following Eq. (3).

**Table 2** Isothermal crystallization kinetic parameters of neat PLA and nucleated PLA/PBAT blend films with talc and MDI

Samples	Data	$T_c/^\circ\text{C}$						$\Delta E_a/\text{kJ mol}^{-1}$
		100	105	110	115	120	125	
PLA	$K/10^{-4} \text{ min}^{-n}$	350.41	192.40	113.36	92.41	75.82	27.33	-595.30
	$n$	2.20	2.39	2.36	2.20	2.35	2.42	
	$t_{1/2}/\text{min}$	4.3	5.0	5.3	5.3	5.5	6.7	
PLA_PB 90_10	$K/10^{-4} \text{ min}^{-n}$	643.95	298.24	344.02	267.08	230.66	127.55	-514.94
	$n$	2.74	2.54	2.44	2.49	2.33	2.35	
	$t_{1/2}/\text{min}$	2.2	3.2	3.5	3.6	4.4	5.9	
PLA_PB_Ta 90_10_1	$K/10^{-4} \text{ min}^{-n}$	1067.62	1037.54	886.79	857.92	555.01	651.52	-250.14
	$n$	2.62	2.64	2.68	2.45	2.45	2.41	
	$t_{1/2}/\text{min}$	1.9	2.0	2.0	2.2	2.6	2.7	
PLA_PB_Ta_MD 90_10_1_1	$K/10^{-4} \text{ min}^{-n}$	1290.33	767.01	623.24	631.03	590.77	356.66	-304.75
	$n$	2.66	2.69	2.79	2.58	2.43	2.70	
	$t_{1/2}/\text{min}$	2.1	2.2	2.3	2.4	2.6	2.8	
PLA_PB_Ta_MD 90_10_1_3	$K/10^{-4} \text{ min}^{-n}$	754.75	436.98	469.03	573.72	334.87	260.36	-312.20
	$n$	2.66	2.74	2.69	2.45	2.62	2.37	
	$t_{1/2}/\text{min}$	2.1	2.6	2.6	2.7	3.4	3.6	
PLA_PB_Ta_MD 90_10_1_5	$K/10^{-4} \text{ min}^{-n}$	472.62	510.96	441.34	260.84	264.76	214.76	-325.27
	$n$	2.63	2.42	2.60	2.72	2.47	2.40	
	$t_{1/2}/\text{min}$	2.7	2.8	2.8	3.7	4.0	4.1	
PLA_PB_Ta_MD 90_10_1_7	$K/10^{-4} \text{ min}^{-n}$	382.49	509.19	269.01	316.86	184.09	167.79	-354.53
	$n$	2.79	2.53	2.70	2.64	2.62	2.43	
	$t_{1/2}/\text{min}$	2.6	2.7	3.2	3.3	4.0	4.3	

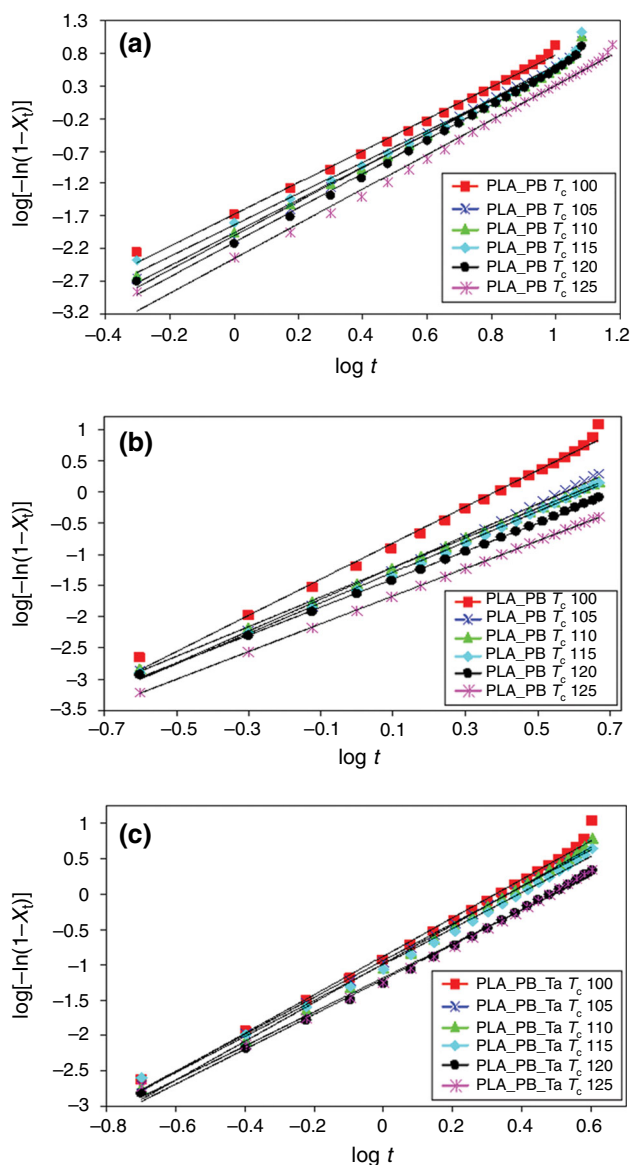


**Fig. 6** Avrami plots of **a** neat PLA, **b** PLA/PBAT (90/10), and **c** PLA/PBAT/talc (90/10/1) blend films for isothermal crystallization at different crystallization temperatures

$$\log[-\ln(1 - X_t)] = n \log t + \log K \quad (3)$$

The plots of  $\log[-\ln(1 - X_t)]$  as a function of  $\log t$  can be used to determine the important kinetic parameters,  $n$  and  $K$ , from slope and intersection point with  $Y$  axis according to linear expression, respectively. Figure 6 shows the plots of  $\log[-\ln(1 - X_t)]$  as a function of  $\log t$  of neat PLA, PLA/PBAT (90/10 w/w) blend films with and without talc. All crystallization kinetic parameters and  $t_{1/2}$  of neat PLA and its blends are listed in Table 2. The  $n$  value of neat PLA was about 2.20–2.42, while that of nucleated PLA/PBAT (90/10 w/w) blends with and without talc were about 2.33–2.74 and 2.41–2.68, respectively. In addition, the PLA/PBAT/talc blends with different MDI

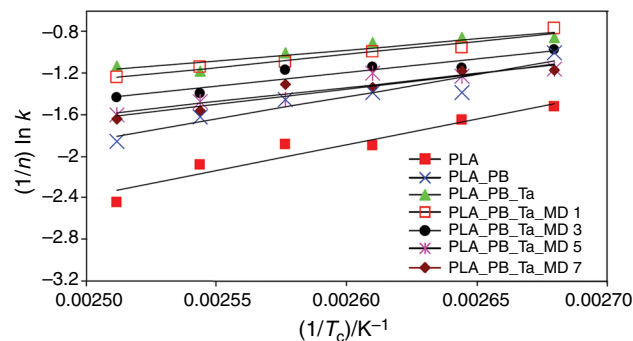


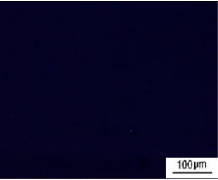
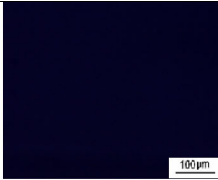
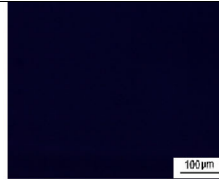
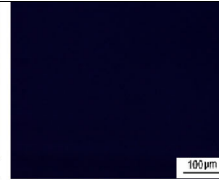
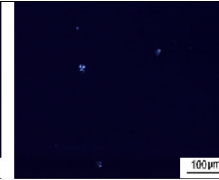
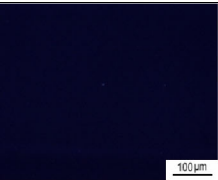
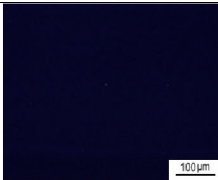
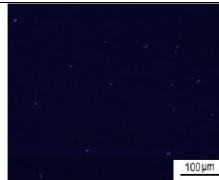
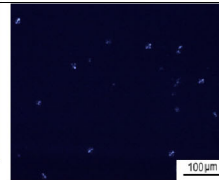
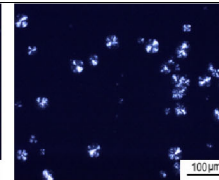
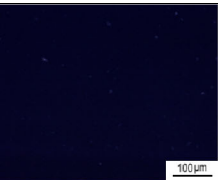
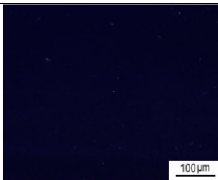
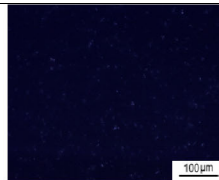
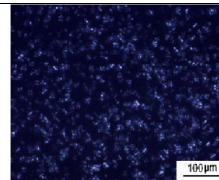
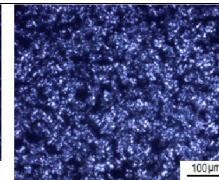
**Fig. 7** Plots of  $(1/n)\ln k$  as a function of  $1/T_c$  of neat PLA and nucleated PLA blend films with and without MDI content for isothermal crystallization

contents displayed the range of  $n$  value between 2.42 and 2.79, indicating that the presence of PBAT, talc, and/or MDI led to the increment of  $n$  value of PLA. As shown in Table 2, the  $n$  value of neat PLA was closed to 2 representing the dimensionability of circular disk shape growth; on the other hand, the  $n$  values of all nucleated PLA blends were almost 3 suggesting the dimensionability of spherical growth [4]. The various amounts of MDI were hardly affected to the  $n$  values of the nucleated PLA blend films compared with neat PLA. Furthermore, the increment of  $n$  value in nucleated PLA blend films indicated that the chain folding crystallization mechanism of PLA was affected by the addition of PBAT, talc, and MDI.

The  $K$  values which were the crystallization rate constant can be used to evaluate the rate of crystallization of the neat PLA and its blends. Table 2 illustrates the  $K$  values which were affected by the different  $T_c$ s and presence of additives into the blends. At all conditions, the  $K$  values were obviously decreased with an increasing of  $T_c$  from 100 to 125 °C, indicating that for isothermal crystallization, a slower rate of crystallization can be observed with higher  $T_c$ . Besides, these results showed the increment of  $K$  values in the following orders from neat PLA, PLA/PBAT, and PLA/PBAT/talc blend films, respectively. Nonetheless, the increasing of MDI amount (0–7 mass%) on the nucleated PLA blends led to the reducing  $K$  values at all ranges of isothermal  $T_c$  (100–125 °C). For instance, the  $K$  value of neat PLA increased around ninefold compared to that of PLA/PBAT/talc blend films at  $T_c$  of 115 °C, indicating that the addition of PBAT and talc can improve the isothermal crystallization of PLA and at the same time talc can be used as an effective nucleating agent for PLA. On the other hand, the  $K$  value of nucleated PLA blend films with 7 mass% MDI was decreased about threefold compared to that of blend films without MDI at  $T_c$  of 115 °C. These experimental values were consistent with the results of  $t_{1/2}$ , crystallization rate, and polarized optical micrographs.



**Table 3** Polarized optical micrographs of neat PLA and nucleated PLA/PBAT (90/10) blend films with and without talc after isothermal crystallization at 115 °C

Sample ID	Time/min				
	0	1	3	5	10
PLA					
PLA_PB 90_10					
PLA_PB_Ta 90_10_1					

The  $n$ ,  $K$ , and  $T_c$  values from crystallization kinetic studies were used to calculate the activation energy of isothermal crystallization processes by following the Arrhenius equation form [11].

$$\left(\frac{1}{n}\right) \ln K = \ln K_0 - \frac{\Delta E_a}{RT_c} \tag{4}$$

where  $K_0$  is the temperature-dependent pre-exponential factor,  $\Delta E_a$  is the activation energy,  $R$  is the gas constant, and  $T$  is the absolute temperature. Figure 7 shows the plots of  $(1/n)\ln K$  as a function of  $1/T_c$  which can be used to determine the  $\Delta E_a$  for each sample. As listed in Table 2, for isothermal crystallization at  $T_c$  ranging from 100 to 125 °C, the  $\Delta E_a$  values of neat PLA, nucleated PLA/PBAT blend films with and without talc were about  $-595$ ,  $-515$ , and  $-250$   $\text{kJ mol}^{-1}$ , respectively. Generally, the minus signal of energy value means the exothermic reaction which indicates the crystal forming in crystallization processes. These kinetic results suggested that the crystallization process of PLA was more difficult than that of PLA/PBAT blends with and without talc, which are also in agreement with  $t_{1/2}$  values. In cases of the influence of MDI levels, the  $\Delta E_a$  values of the nucleated PLA/PBAT/talc blend films with various MDI contents were in the range of  $-305$  to  $-354$   $\text{kJ mol}^{-1}$  which were higher than those without MDI ( $-250$   $\text{kJ mol}^{-1}$ ), implying that the presence of MDI into the blend films retarded the crystallization of

the PLA. Furthermore, the increasing MDI contents led to a slower crystallization rate of the blend films. To confirm these results from behaviors and kinetics of crystallization, POM technique was used to follow up the morphological and crystallization changes in neat PLA and its blends.

### Spherulitic density and crystallization

The spherulitic morphology and crystallization behaviors of PLA and its blends were isothermally investigated at  $T_c$  of 115 °C by polarized optical microscope (POM) technique. Table 3 shows the polarized optical micrographs of neat PLA and nucleated PLA/PBAT (90/10 w/w) blend films with and without talc after isothermal crystallization at 115 °C. Generally, neat PLA has low crystallinity and slow crystallization rate which can be noticed from its POM images. After isothermal crystallization for 5 min, the spherulitic growth on neat PLA was slightly formed. However, nucleation density of neat PLA and its blends was obviously observed with the increment of isothermal crystallization time. In addition, these results revealed that the nucleation density of PLA/PBAT (90/10 w/w) blend films significantly increased compared to that of the neat PLA at the same isothermal crystallization time, indicating that the presence of PBAT prompted the spherulitic growth of PLA.

**Table 4** Polarized optical micrographs of nucleated PLA/PBAT/talc (90/10/1) blend films at different MDI contents after isothermal crystallization at 115 °C

Sample ID	Time/min				
	0	1	3	5	10
PLA_PB_Ta_MD 90_10_1_1					
PLA_PB_Ta_MD 90_10_1_3					
PLA_PB_Ta_MD 90_10_1_5					
PLA_PB_Ta_MD 90_10_1_7					

Similar results have been reported by Xiao et al. [27]. They studied the isothermal crystallization behaviors of PLA blends with various PBAT contents at crystallization temperature range of 123–142 °C. The results illustrated that blending PLA with PBAT can improve the crystallization rate but almost did not change the crystallization mechanism of PLA. They explained that the increasing crystallization rate of PLA/PBAT blends might be resulting from the immiscibility of PLA and PBAT which provided convenient nucleation sites for PLA isothermal crystallization. Furthermore, PLA blending with the other flexible polymers such as PCL and PES also led to an enhancing of crystallization rate with the increasing flexible polymer amounts [28].

In addition, Table 3 displays and confirms the synergistic effect of PBAT and talc on isothermal crystallization of PLA. The presence of PBAT and talc in the PLA blends resulted in the remarkable increment of crystallization rate and nucleation density of PLA. It could be clearly observed from POM images of PLA/PBAT (90/10 w/w) blend films with and without talc after isothermal crystallization time of 5 min compared to that of neat PLA. These POM results exhibited that talc, acted as a nucleating agent, played an

important role together with PBAT to develop a large number of nuclei into melted polymer matrix leading to tiny and more spherulites. It could be claimed that synergism between PBAT and talc has been occurred which is in agreement with crystallization behaviors and kinetics investigated by DSC analysis. These results can be summarized that on the one hand the addition of PBAT and talc can accelerate the rate of crystallization, but on the other hand, talc directly affects smaller size of spherulite.

The influence of MDI levels (0–7 mass% based on PBAT content) on the nucleated PLA/PBAT/talc (90/10/1 w/w) blend films after isothermal crystallization at 115 °C is presented in Table 4. Interestingly, when the MDI amounts increased, nucleation density of the nucleated PLA blends was reduced; in contrast, spherulitic size was extended. In other words, it means that the crystallization rate of nucleated PLA blend films was retarded with the increasing MDI levels. These behaviors were evidently appeared after isothermal crystallization at 115 °C for 5 min. For example, the polarized optical micrographs of nucleated blend films with lower MDI contents (1 and 3 mass% MDI) still displayed the smaller and denser spherulites. On the other

hand, these with higher MDI amounts (5 and 7 mass%) showed the disappearance of nucleation density under the same condition. It could be claimed with a reasonable assumption that MDI with a highly reactive functional groups might acted as a chain extender between PLA and PBAT which then led to a longer polymer chain lengths and/or chain branches, inhibiting the possibility of forming chain-folded lamellar structure of PLA because the increment of chain length and/or chain rigidity significantly affected polymer crystallization processes. This is a reason why the more MDI contents added the higher possibility of polymer chain length expanded. Thus, the rate and density of crystallization for nucleated PLA blend films with MDI were lower than those without MDI. These behaviors are consistent with the involved kinetic parameters ( $t_{1/2}$ ,  $K$ , and  $\Delta E_a$ ) in isothermal crystallization studies (Table 2).

## Conclusions

Melt crystallization behaviors and kinetics of neat PLA and its blends were isothermally investigated at the  $T_c$  range of 100–125 °C. DSC curves revealed a synergistic effect of PBAT and talc on the faster crystallization rate of PLA. In contrast, the influence of MDI on the PLA blend films retarded the rate of crystallization depending on the MDI levels. The crystallization rate was apparently decreased with increasing  $T_c$ . Furthermore, the crystallization behaviors of neat and nucleated PLA blend films were also confirmed by  $t_{1/2}$  values which were inversely proportional to crystallization rate. These results were consistent with crystallization kinetic and morphological studies. The  $n$  and  $K$  values of PLA increased evidently with the presence of PBAT, talc, and various levels of MDI at all conditions; in contrast, the  $\Delta E_a$  values decreased progressively. The POM images indicated the increasing of nucleation density and spherulitic growth with the addition of PBAT and talc, revealing that talc acted as an effective nucleating agent for PLA and played an important role together with PBAT to develop a large number of nuclei into melted PLA matrix. However, nucleation density of the nucleated PLA blends was reduced with the increasing of MDI contents which might be occurred from longer chain length and higher chain rigidity leading to hindered crystallization of the blends.

**Acknowledgements** The authors acknowledged the financial support from Ratchadapiseksomphot Endowment Fund, Chulalongkorn University (Sci-Super 2014-030) and The 90th Anniversary of Chulalongkorn University Fund. Additionally, this research was partially supported by Ratchadapiseksomphot Endowment under Outstanding Research Performance Program (GF\_58\_08\_23\_01). W. Phetwarotai gratefully thanks the Development and Promotion of Science and Technology Talents project (DPST).

## References

1. Re GL, Benali S, Habibi Y, Raquez JM, Dubois P. Stereocomplexed PLA nanocomposites: from in situ polymerization to materials properties. *Eur Polym J*. 2014;54:138–50.
2. Martin O, Averous L. Poly(lactic acid): plasticization and properties of biodegradable multiphase systems. *Polymer*. 2001;42:6209–19.
3. Kelnar I, Kratochvil J, Kapralkova L. Crystallization and thermal properties of melt-drawn PCL/PLA microfibrillar composites. *J Therm Anal Calorim*. 2016;124:799–805.
4. Hwang JJ, Huang SM, Liu HJ, Chu HC, Lin LH, Chung CS. Crystallization kinetics of poly(L-lactic acid)/montmorillonite nanocomposites under isothermal crystallization condition. *J Appl Polym Sci*. 2012;124:2216–26.
5. Wang Y, Chiao SM, Hung TF, Yang SY. Improvement in toughness and heat resistance of poly(lactic acid)/polycarbonate blend through twin-screw blending: influence of compatibilizer type. *J Appl Polym Sci*. 2012;125:E402–12.
6. Zhang N, Wang Q, Ren J, Wang L. Preparation and properties of biodegradable poly(lactic acid)/poly(butylene adipate-co-terephthalate) blend with glycidyl methacrylate as reactive processing agent. *J Mater Sci*. 2009;44:250–6.
7. Arrieta MP, Lopez J, Hernandez A, Rayon E. Ternary PLA–PHB–limonene blends intended for biodegradable food packaging applications. *Eur Polym J*. 2014;50:255–70.
8. Arrieta MP, Lopez J, Ferrandiz S, Peltzer MA. Characterization of PLA–limonene blends for food packaging applications. *Polym Test*. 2013;32:760–8.
9. Shi N, Dou Q. Non-isothermal cold crystallization kinetics of poly(lactic acid)/poly(butylene adipate-co-terephthalate)/treated calcium carbonate composites. *J Therm Anal Calorim*. 2015;19: 635–42.
10. Henricks J, Boyum M, Zheng W. Crystallization kinetics and structure evolution of a polylactic acid during melt and cold crystallization. *J Therm Anal Calorim*. 2015;120:1765–74.
11. Xiao HW, Li P, Ren X, Jiang T, Taut YJ. Isothermal crystallization kinetics and crystal structure of poly(lactic acid): effect of triphenyl phosphate and talc. *J Appl Polym Sci*. 2010;118:3558–69.
12. Liao HT, Wu CS. Preparation and characterization of ternary blends composed of polylactide, poly( $\epsilon$ -caprolactone) and starch. *Mat Sci Eng A Struct*. 2009;515:207–14.
13. Zhang JF, Sun X. Mechanical and thermal properties of poly(lactic acid)/starch blends with dioctyl maleate. *J Appl Polym Sci*. 2004;94:1697–704.
14. Shin BY, Jo GS, Kim BS, Hong KH, Cho BH. Properties of compatibilized PLA/starch blends. *Appl Chem*. 2006;10:77–88.
15. Jang WY, Shin BY, Lee TJ, Narayan R. Thermal properties and morphology of biodegradable PLA/starch compatibilized blends. *J Ind Eng Chem*. 2007;13:457–64.
16. Carson D, Nie L, Narayan R, Dubois P. Maleation of polylactide (PLA) by reactive extrusion. *J Appl Polym Sci*. 1999;72:477–85.
17. Plackett D. Maleated polylactide as an interfacial compatibilizer in biocomposites. *J Polym Environ*. 2004;12:131–8.
18. Wang H, Sun X, Seib P. Strengthening blends of poly(lactic acid) and starch with methylenediphenyl diisocyanate. *J Appl Polym Sci*. 2001;82:1761–7.
19. Wang H, Sun X, Seib P. Effect of starch moisture on properties of wheat starch and poly(lactic acid) blend containing methylenediphenyl diisocyanate. *J Polym Environ*. 2002;10:133–8.
20. Phetwarotai W, Potiyaraj P, Aht-Ong D. Properties of compatibilized polylactide blend films with gelatinized corn and tapioca starches. *J Appl Polym Sci*. 2010;116:2305–11.
21. Li H, Huneault MA. Effect of nucleation and plasticization on the crystallization of poly(lactic acid). *Polymer*. 2007;48:6855–66.

22. Lee JH, Jeong YG. Preparation and crystallization behavior of polylactide nanocomposites reinforced with POSS-modified montmorillonite. *Fibers Polym.* 2010;12:180–9.
23. Phetwarotai W, Aht-Ong D. Properties and nonisothermal crystallization behavior of nucleated polylactide biodegradable composite films. *Adv Mater Res.* 2012;488:671–5.
24. Jiang XL, Luo SJ, Sun K, Chen XD. Effect of nucleating agents on crystallization kinetics of PET. *Express Polym Lett.* 2007;1:245–51.
25. Phetwarotai W, Aht-Ong D. Reactive compatibilization of polylactide, thermoplastic starch and poly(butylene adipate-co-terephthalate) biodegradable ternary blend films. *Mater Sci Forum.* 2011;695:178–81.
26. Gedde UFLW. *Polymer physics.* 1st ed. London: Chapman & Hall; 1995.
27. Xiao H, Lu W, Yeh JT. Crystallization behavior of fully biodegradable poly(lactic acid)/poly(butylene adipate-co-terephthalate) blends. *J Appl Polym Sci.* 2009;112:3754–63.
28. Dell’Erba R, Groeninckx G, Maglio M, Malinconico M, Migliozzi A. Immiscible polymer blends of semicrystalline biocompatible components: thermal properties and phase morphology analysis of PLLA/PCL Blends. *Polymer.* 2001;42:7831–40.